

Influence of Fiber Length on Mechanical Properties of Fabric Reinforced C/C-SiC

Christian Zuber, Thomas Reimer
DLR – German Aerospace Center
Institute of Structures and Design
D-70569 Stuttgart

Introduction

DLR is responsible for the manufacturing of the CMC nose cap for the ESA aerothermodynamic experimental vehicle EXPERT [1]. The challenge was to manufacture a large (diameter: 700 mm, height: 450 mm) nose cap structure [2] with integrated load introduction elements via the liquid silicon infiltration process (LSI) developed by DLR [3]. The LSI process is divided into three main steps - the CFRP manufacturing, the pyrolysis and the siliconizing. During pyrolysis of the CFRP component the polymer matrix is converted to amorphous carbon which goes along with large volume shrinkage of the matrix. However, since the fibers are not affected by the pyrolysis and do not shrink, the macroscopic component shrinkage for the 2-D case is limited effectively to the laminate transversal direction. In the case where a multi-curvature component is processed, the anisotropic shrinkage can lead to high internal stresses. To reduce these internal stresses, which can cause delaminations on such parts during pyrolysis, the CFRP lay-up was modified in the present case. The size of the prepreg patches was adapted, the fiber orientation was varied and the fiber length in the fabric layers was shortened with a cutting tool. In this paper the influence of the fiber length on the mechanical properties of the CMC is presented.

Sample manufacturing

To investigate the influence of the fiber length on the mechanical properties of the CMC, two plates with projected 300 x 300 x 5 mm³ in C/C-SiC with endless as well as with cut fibers were made via the Liquid Silicon Infiltration (LSI) process (Table 1).

Table 1: Test plate overview

| plate | reinforcement | precursor | fibre orientation | fibre cutting |
|-------|---------------|---------------------|-------------------|---------------|
| HP393 | HTA fabric | JK60 phenolic resin | 0°/90° | no |
| HP394 | HTA fabric | JK60 phenolic resin | 0°/90° | 0° & 90° |

In general the LSI process can be split into three major steps (Figure 1). Basically the process starts with the fabrication of a carbon fiber reinforced plastic (CFRP) composite. It's essential to use phenolic precursor matrices of high carbon yield. After curing, the composites are tempered for 4 h at 240 °C to complete the polymerization of the matrix as well as to initiate first matrix cracks. Subsequently, these CFRP composites are pyrolyzed in a two step process. Firstly the CFRP composites are pyrolyzed under inert atmosphere (e.g. nitrogen) at a temperature of 900 °C to convert the polymer matrix to amorphous carbon. Afterwards the C/C composites are heat-treated under vacuum at a temperature of 1650 °C. The pyrolysis of the polymer matrix leads to a macroscopic shrinkage and forms a microscopic network of cracks within the resulting C/C composites. The siliconizing is the third and final processing step. During the siliconizing the capillary effect of the trans-laminar crack system and the low viscosity of the molten silicon enable a quick filling of the micro cracks with molten silicon. The exothermic reaction between the carbon matrix and the molten silicon results in silicon carbide which encapsulates the carbon/carbon bundles. The siliconizing takes place under vacuum at a temperature of 1650 °C.

The C/C-SiC composites in principle comprise three phases. These are the carbon phase consisting of carbon fibers and residual carbon matrix, silicon carbide and a small share of unreacted silicon.

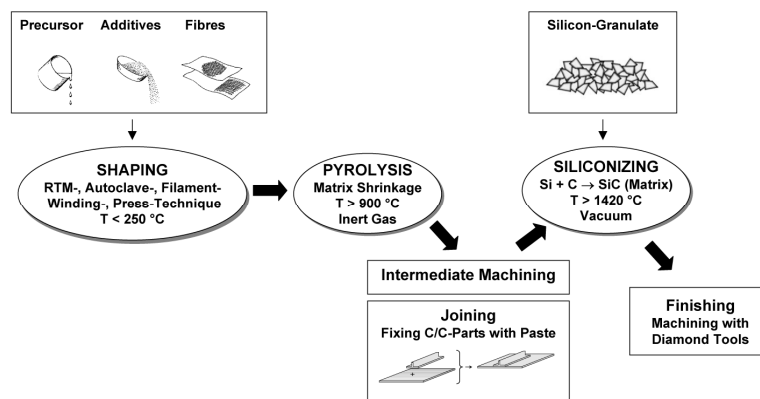


Figure 1: Liquid Silicon Infiltration (LSI) process

During the first process step the CFRP green bodies of the sample plates were made by warm pressing technique. The pressing cycle was adapted from the autoclave cycle used for the manufacturing of the nose cap green body. To reduce the effective fiber length of plate HP394, the same die cutting tool was used as for the nose cap pre-cut prepreg parts. The resulting maximum fiber length was 30 mm. After pyrolysis and siliconization, tensile

specimens were cut out of the test plates by water jet cutting in $0^\circ/90^\circ$ and $\pm 45^\circ$ direction. In Figure 2 the dimensions of the tensile specimens are given.

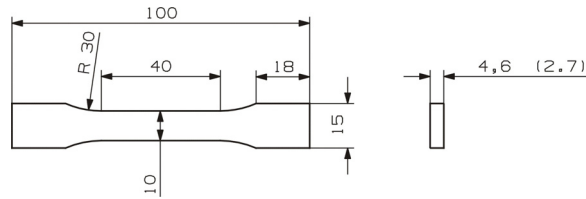


Figure 2: Tensile specimen dimensions

Already in the CFRP stage a kind of blurring of the $0^\circ/90^\circ$ fiber orientation was visible in the sample plate with cuts. To analyze the degree of the fiber displacement, one tensile specimen was inspected via computer tomography (CT). Figure 3 shows the displacement of the $0^\circ/90^\circ$ fiber orientation caused by the fiber cutting in combination with the warm pressing.

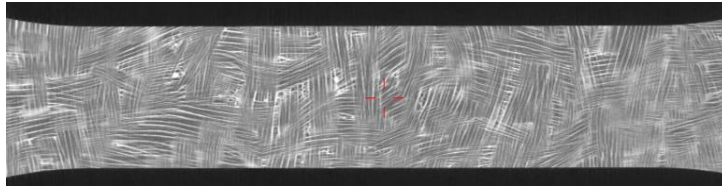


Figure 3: CT Inspection of tensile specimen

For the calculation of the Young's modulus accurate strain values were needed. Therefore each tensile specimen was equipped with a strain gauge on each side. During the test result interpretation, the strain gauge data was used to calculate the "edge values" based on the stress and strain values. The "edge values" incorporate the bending influence and therefore the multi axial load case which could be observed during the tensile tests.

Experimental Results

The tensile tests were conducted according to DIN EN 658-1 [4] using a Zwick 1475 testing machine.

Plate HP393 – reference material based on uncut fabrics

With an average ultimate stress of $\sigma_{\text{ultimate,edge } 0^\circ/90^\circ} = 136.4 \text{ MPa}$ (Table 2, number of specimen used for averaging is indicated at the corresponding diagram) the uncut reference material showed properties known from standard material made by autoclave technique. While the ultimate strain values

in $0^\circ/90^\circ$ direction were in the expected range of $\epsilon_{\text{ultimate,edge } 0^\circ/90^\circ} = 2.43 \text{ ‰}$ on average, the ultimate strain values in $\pm 45^\circ$ direction were considerably higher with $\epsilon_{\text{ultimate,edge } \pm 45^\circ} = 10.44 \text{ ‰}$ (Figure 4 and Figure 5).

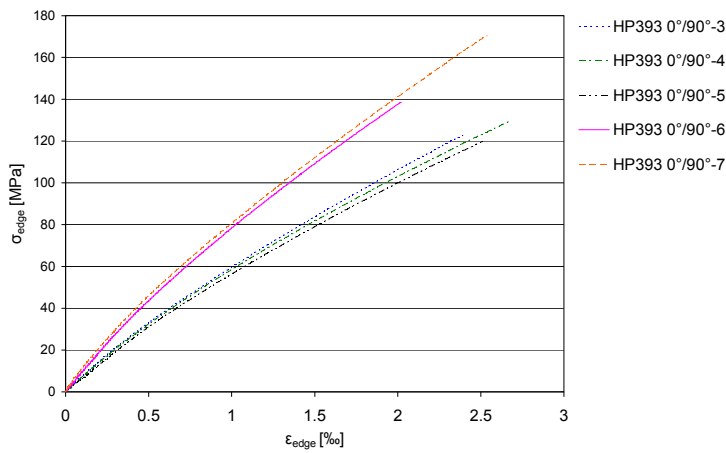


Figure 4: Tensile strength / strain diagram (HP393, $0^\circ/90^\circ$ fiber orientation)

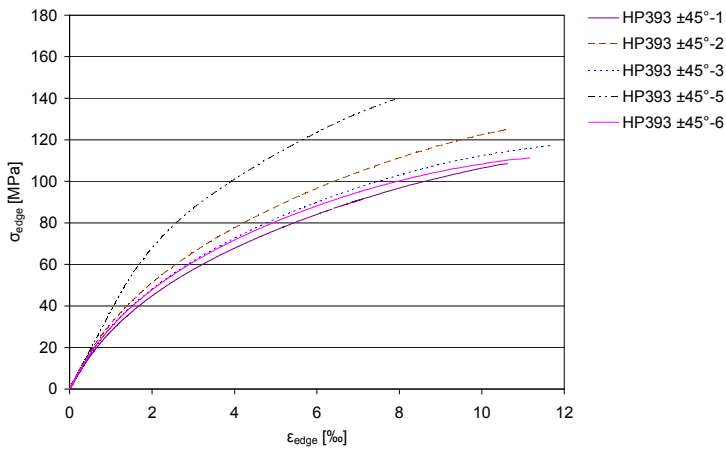


Figure 5: Tensile strength / strain diagram (HP393, $\pm 45^\circ$ fiber orientation)

Plate HP394 – cut fiber fabrics (fiber length 30mm)

The results for the tensile test of the modified material showed a high variance of the maximum tensile strength values (Figure 6 and Figure 7). As a result of fiber cutting and the fiber displacement, the material had a reduced average ultimate stress of $\sigma_{\text{ultimate,edge } 0^\circ/90^\circ} = 80.0 \text{ MPa}$, which is 41.3 % lower

compared to the reference material (Figure 6). In $\pm 45^\circ$ fiber direction an average ultimate stress of $\sigma_{\text{ultimate,edge } \pm 45^\circ} = 76.67 \text{ MPa}$ was measured. Young's modulus for the $0^\circ/90^\circ$ and $\pm 45^\circ$ fiber orientation was in the same range as for the uncut reference material (Table 2). Also mentionable were the ultimate strain values with $\epsilon_{\text{ultimate,edge } 0^\circ/90^\circ} = 1.84 \text{ ‰}$ in $0^\circ/90^\circ$ and $\epsilon_{\text{ultimate,edge } \pm 45^\circ} = 3.81 \text{ ‰}$ in $\pm 45^\circ$ fiber direction. They were much more similar to each other, compared to the uncut reference material, which showed a factor of more than four between $\epsilon_{\text{ultimate,edge } 0^\circ/90^\circ}$ and $\epsilon_{\text{ultimate,edge } \pm 45^\circ}$.

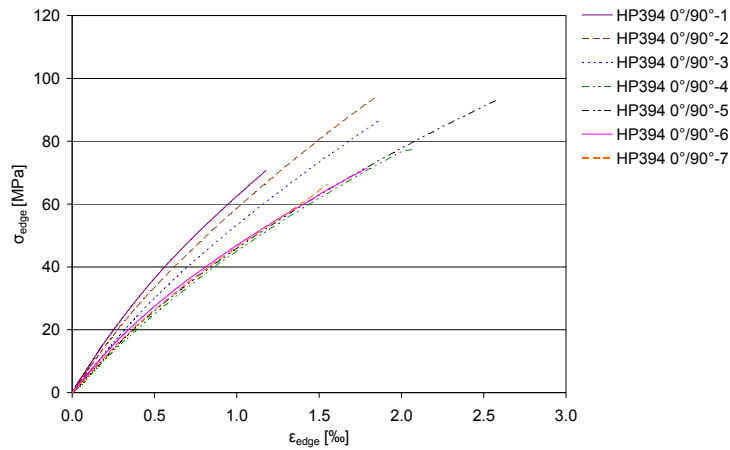


Figure 6: Tensile strength / strain diagram (HP394, $0^\circ/90^\circ$ fiber orientation)

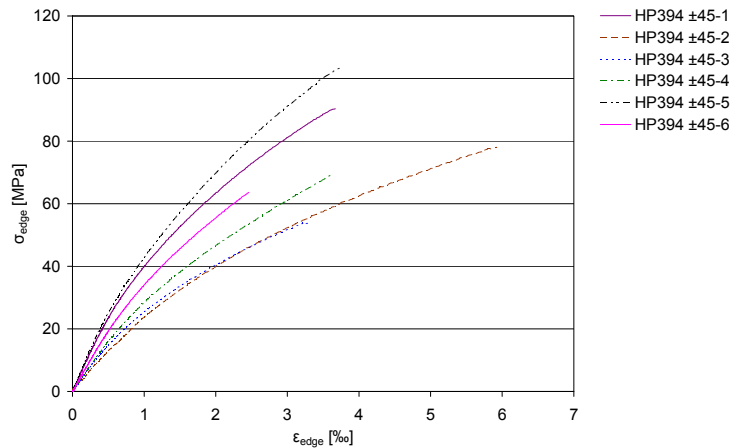


Figure 7: Tensile strength / strain diagram HP394 ($\pm 45^\circ$ fiber orientation)

Table 2: Tensile test results

| plate | fibre orientation | $\sigma_{ultimate}$ [MPa] | $\sigma_{ultimate,edge}$ [MPa] | Young's modulus [GPa] | ϵ_{edge} [‰] |
|-------|-------------------|---------------------------|--------------------------------|-----------------------|-----------------------|
| HP393 | 0°/90° | 120.6 (s = 5.5) | 136.4 (s = 20.3) | 77.7 (s = 15.5) | 2.43 (s = 0.52) |
| | ±45° | 95.1 (s = 1.1) | 120.2 (s = 12.4) | 34.0 (s = 2.5) | 10.44 (s = 1.50) |
| HP394 | 0°/90° | 69.2 (s = 9.8) | 80 (s = 11.3) | 63.6 (s = 10.0) | 1.84 (s = 0.50) |
| | ±45° | 56.7 (s = 7.8) | 76.7 (s = 18.1) | 38.5 (s = 11.2) | 3.82 (s = 1.17) |

Conclusions

While the fiber length reduction worked well for the nose cap, which means no fiber displacement could be observed, it caused problems during the CFRP manufacturing of the test plate. The cut fabric showed heavy fiber displacement due to the warm pressing. The observed mechanical weakening of the samples is caused in part by the fiber displacement.

The reference material showed high ultimate strain values in ±45° direction ($\epsilon_{ultimate,edge \pm 45^\circ} = 10.44$ ‰) and a high influence of the fiber orientation ($\epsilon_{ultimate,edge 0^\circ/90^\circ} = 2.43$ ‰). Whereas the ultimate strain values for the modified material based on cut fabrics ($\epsilon_{ultimate,edge 0^\circ/90^\circ} = 1.84$ ‰ and $\epsilon_{ultimate,edge \pm 45^\circ} = 3.81$ ‰) were lower and much closer together. This was explained by the reduced load transfer between the cut C/C bundles, which yield a more matrix-dominated material behavior. Due to the fact that the maximum calculated stress values of the nose cap are between 20 – 30 MPa there is still a considerable margin even with the reduced strength values.

References

- [1] J. Gavira, "EXPERT - A European Aerothermodynamics In-Flight Testbed", Proceedings 6th European Workshop on Thermal Protection Systems and Hot Structures, 1-3 April 2009, Stuttgart, Germany
- [2] T. Reimer, K. Stubicar, G. Koppenwallner, R. Müller-Eigner, S. Lein, A. Steinbeck, "Overview about the Instrumented Nose Assembly Development for the EXPERT Capsule", 16th AIAA International Space Planes and Hypersonic Systems and Technologies Conference, 19-22 Oct. 2009, Bremen, Germany
- [3] W. Krenkel, "Entwicklung eines kostengünstigen Verfahrens zur Herstellung von Bauteilen aus keramischen Verbundwerkstoffen", Dissertation Universität Stuttgart, DLR-Forschungsbericht 2000-04, Stuttgart, Germany, 2000
- [4] DIN EN 658-1 Januar 1999. Mechanische Eigenschaften von keramischen Verbundwerkstoffen bei Raumtemperatur